Effective Elastic Modulus as a Function of Angular Leaf Span for Curved Leaves of Pyrolytic Boron Nitride

M. L. Kaforey[a], C. W. Deeb[a], & D. H. Matthiesen[a]

Department of Materials Science & Engineering
Case Western Reserve University
Cleveland, OH 44106

Abstract:

A theoretical equation was derived to predict the spring constant (load/deflection) for a simply supported cylindrical section with a line force applied at the center. Curved leaves of PBN were mechanically deformed and the force versus deflection data was recorded and compared to the derived theoretical equation to yield an effective modulus for each leaf. The effective modulus was found to vary from the pure shear modulus for a flat plate to a mixed mode for a half cylinder as a function of the sine of one half the angular leaf span. The spring constants of individual PBN leaves were usually predicted to within 30%.

NAG 8 - 1268
PREPRINT
IN / 39

1. Introduction

Springs composed of stacks of curved leaves of pyrolytic boron nitride (PBN) have been used in microgravity experiments dealing with solidification processing of semiconductors[1-4]. The springs were used to accommodate the volume change due to the shrinkage of the semiconductor upon melting. It would be very beneficial to be able to predict the behavior of a spring prior to testing based on its geometry. Thus, an equation for the deformation of a cylindrical section was derived. The use of this equation requires knowledge of the elastic modulus. However, for PBN, the choice of an appropriate modulus is not trivial.

PBN is a highly anisotropic material with a hexagonal crystal structure having a c/a ratio of approximately 2.66 (calculated using lattice parameter values from Pease[5]). When produced by chemical vapor deposition, the microstructure generally consists of thin, flat plates with the c-axis perpendicular to the substrate surface[6]. Thus, the c-axis will be perpendicular to the surface of curved leaves of PBN produced by chemical vapor deposition.

Experiments using a flat plate of PBN with the c-axis perpendicular to the broad face of the sample were performed and reported in Deeb[7] and Kaforey et al.[8]. Three-point bending was used to measure an elastic modulus of 2.60 ± 0.31 GPa. The mechanism of deformation was believed to be shear between the pyrolytic layers, so this value was assigned to c_{44}.

For the case of curved leaves, the mechanism of deformation is believed to be a combination of shear between the pyrolytic layers (c_{44}) and compression parallel to the layers, that is, within the basal plane (c_{11}). The c_{11} value has been reported to be 750 GPa (Jager[9]) and 830 GPa (Kelly[10]). However, these values are the values intrinsic to the hexagonal crystal structure. Advanced Ceramics[11] and Archer[12] have both tested plates of PBN in compression

with the compression direction being parallel to the layers. They reported values for $E_{//a}$ of 22 and 19.6 GPa, respectively. These measure the bulk material and are much more appropriate for the case of curved leaves. They represent the behavior that would occur in the very edge of a curved leaf that was a full half cylinder. The current work will measure the effective modulus for a half cylinder and for intermediate cases of leaves with various angular leaf spans.

2. Derivation of the theoretical equation for the deflection of a cylindrical section simply supported at opposite edges with a line force applied at the center

Exact solutions are known for the deflection of a flat plate and a half cylinder which are simply supported at opposite sides with a line force applied at the center. Solutions to these and many other cases may be found in Young[13] and Timoshenko & Woinowsky-Krieger[14]. However, the intermediate case of just a portion of a cylinder is not available in the literature. This intermediate case is the situation found in a curved leaf.

From a cylinder of radius, r, a section is cut having a width, w, a depth, b, and a thickness, h, as shown in Figure 1. The section has an angular leaf span, θ, where

$$\theta = 2\arcsin\left(\frac{w}{2r}\right) \tag{1}$$

Also shown on the figure is the line force applied at the center and the support at the edges of the section.

For the cylindrical section, the arc length, $a(x)$, at any point along the section is

$$a(x) = r\left[\arcsin\left(\frac{-\frac{w}{2}+x}{r}\right) - \arcsin\left(\frac{-\frac{w}{2}}{r}\right)\right] \tag{2}$$

3

Considering only one half of the section, since it is symmetrical about the centerline, evaluating equation (2) gives

$$a_{min} = 0 \text{ and } a_{max} = r \arcsin\left(\frac{w}{2r}\right) \tag{3}$$

when $x = 0$ and $x = \frac{w}{2}$, respectively.

Rearranging equation (2) to find $x(a)$ gives the perpendicular distance to any point on the cylindrical section from the plane of the applied force as

$$x(a) = \frac{1}{2}\left\{w + 2r \sin\left[\frac{a}{r} - \arcsin\left(\frac{w}{2r}\right)\right]\right\} \tag{4}$$

The momentum, M, at any point along the cylindrical section is

$$M = \frac{P}{2}x = \frac{P}{4}\left\{w + 2r \sin\left[\frac{a}{r} - \arcsin\left(\frac{w}{2r}\right)\right]\right\} \tag{5}$$

Castigliano's Theorem[15] states that, in general, the deflection, d, is the partial derivative of energy with respect to the applied force,

$$d = \frac{\partial U}{\partial P} \tag{6}$$

where U is the energy and

$$U_{bending} = \frac{1}{2EI}\int_L M^2 dL \tag{7}$$

where L is the length of interest, E is the modulus, and I is the moment of inertia.

Considering the arclength for one half of the cylindrical section as the length of interest and then adding the 2 halves to get the total energy gives

$$U = \frac{1}{EI} \int_{a_{min}}^{a_{max}} M^2 da = \frac{1}{EI} \int_{0}^{r \arcsin\left(\frac{w}{2r}\right)} \frac{P^2}{16} \left\{ w + 2r \sin\left[\frac{a}{r} - \arcsin\left(\frac{w}{2r}\right)\right] \right\}^2 da \quad (8)$$

Integrating and evaluating gives

$$U = \frac{P^2 r}{16EI} \left\{ -4rw + 2rw\sqrt{4 - \frac{w^2}{r^2}} + r^2\theta + \frac{w^2\theta}{2} - r^2 \sin\theta \right\} \quad (9)$$

where θ is the angular leaf span as defined in equation (1). Substituting equation (9) into equation (6) and taking the partial derivative with respect to the applied force gives the deflection of the cylindrical section as

$$d = \frac{Pr}{8EI} \left\{ -4rw + 2rw\sqrt{4 - \frac{w^2}{r^2}} + r^2\theta + \frac{w^2\theta}{2} - r^2 \sin\theta \right\} \quad (10)$$

Equation (10) is the deflection for any cylindrical section of width, w, and radius, r, which is simply supported at opposite edges with a force, P, applied along the centerline.

For dimensions such that the thickness of the section is much smaller that the width (h<<w), the moment of inertia for a rectangular beam (see for example Beer & Johnston[16]) is

$$I = \frac{1}{12} bh^3 \quad (11)$$

Substituting equation (11) into equation (10) and rearranging gives the predicted spring constant, k_p

$$k_p = \frac{P}{d} = \frac{2Ebh^3}{3r\left\{ -4rw + 2rw\sqrt{4 - \frac{w^2}{r^2}} + r^2\theta + \frac{w^2\theta}{2} - r^2 \sin\theta \right\}} \quad (12)$$

5

3. Experimental Procedure

Pyrolytic boron nitride leaves of various angular leaf spans were made by cutting PBN Vertical Bridgman crucibles (Advanced Ceramics Co., Cleveland, OH) using the following procedure. The seedwell and taper were cut from the rest of the crucible, leaving a cylinder of radius, r. The c-axis of the pyrolytic structure is perpendicular to the surface to the cylinder. Strips of width, w, were made by cutting the cylinder lengthwise. The strips were then cut perpendicular to their length to a depth, b. Springs were thinned to the desired thickness by separating the pyrolytic layers with a razorblade.

The leaves were cleaned with acetone after cutting and then baked out in air in a small box furnace at 500°C overnight. In general, the leaves were very white after cleaning with rare cases of residual carbon remaining on the surface.

Half cylinders were obtained by cutting cylinders of PBN lengthwise. After cutting, the samples were examined to insure that the width was equal to the diameter. Due to the residual compressive stresses at the outside surface of the cylinder[17], a new, smaller radius was generally measured, necessitating further processing to obtain exact half cylinders. The edges of the cylinder were lightly ground with 600 grit SiC until enough material was removed to yield a usable half cylinder. The samples were measured again to report the actual radius at the start of testing.

Force versus deflection data for half cylinders and for individual leaves of various angular leaf spans were obtained using a mechanical testing system (Instron Model 1125, Instron Corp., Canton, MA). The radius of curvature for the ram was chosen to be as small as possible to approximate a line force acting on the midpoint of the cylinder width. The radius of the ram was 4 mm.

6

An Instron "B" 2000 gram load cell was used throughout these experiments. This load cell is incompatible with the electronic calibration of the Instron 1125. Dead weight calibration weights of 5 lbs., 2 lbs., 1 lb., and 8 oz were therefore used for the calibration. Although the calibration values did not drift more than 2% between tests, calibration was performed before each experiment to insure accuracy.

The platen was machined from magnesium plate and tapped to fit the thread of the load cell. Magnesium plate was used to add as little weight as possible to the apparatus, effectively increasing the amount of load that could be measured during testing. Between experiments, boron nitride mould release was sprayed on the platen to act as a lubricant. Lubrication was used to conform to the condition that there is no constraint on the contact edges of the leaf.

The samples were loaded at a rate of 0.5 mm/min to a preset deflection, a steady load was attained, and the samples were unloaded. The platen was cleaned of all boron nitride powder remaining from previous tests, and reapplied between tests. The maximum deflection for each case was determined by the more limiting of the maximum deflection to flatten the leaf or the maximum load of the load cell.

The data was recorded directly onto chart paper to obtain continuous data collection. Each cycle consisted of applying a load, pausing until steady state was reached, and unloading the sample. Each sample was cycled a minimum of 7 times and data was recorded for all cycles.

The steady state load, P, and the maximum deflection, d, were measured for and a value for P/d was calculated for each cycle. The first two cycles for each sample were discarded because excessive settling between contact points and sticking between the springs and the spring chamber sometimes occurred in the first two cycles. The remaining 5 cycles were averaged. This resulted in an average spring constant, k, for each experiment ($k=P/d$). An

7

effective modulus was then determined for each experiment using equation (12). For the half

cylinders, rearranging equation (10) reduces to the following equation[14] when the appropriate

limits are considered:

$$E = \left(\frac{3}{8}\pi - 1\right)\frac{P}{d}\frac{r^3}{I}$$ (13)

4. Results

Half Cylinder Experiments

A typical force versus deflection chart recording for one cycle of a half cylinder

experiment is shown in Figure 2. The loading curves increased monotonically. There was a

transient at the beginning of the loading curve that settled into a linear portion as the deflection

increased. There was a small degree of load relaxation after the maximum deflection was

attained. All half cylinder tests reached steady load shortly after reaching the maximum

deflection. The steady state load was determined by holding the spring at the maximum

deflection until the load did not vary with time. This value was then taken as the steady state

load, P. The total deflection, d, was also measured from the chart for each cycle. The spring

constant was calculated for each cycle, the values for the 5 cycles were averaged and the

resulting average for each half cylinder is presented in Table 1. Additionally, the effective

modulus was calculated for each experiment using equation (13) and these results are included in

Table 1. The effective moduli for all of the half cylinders were averaged and the resultant

effective modulus for a half cylinder of PBN was found to be 13.41 ± 2.26 GPa.

Individual Leaf Experiments

A typical force versus deflection chart recording for an individual leaf experiment is shown in Figure 3. The loading curves were all monotonically increasing, exhibiting a loading transient at the onset of deflection, and approaching a linear value as deflection increased. There was a slight load relaxation at maximum deflection. All of the individual spring experiments exhibited the same behavior. The steady state load and maximum deflection were determined as for the half cylinders. The spring constants and effective moduli were calculated using an average of 5 cycles for each of the 18 individual leaf experiments and the results are shown in Table 2.

5. Discussion

Similar curvature was found in force versus deflection curves for flat plates of PBN and of fused quartz[8]. Thus, the initial deviation from linearity was explained as settling of the contact points and the inflection in the unloading curve was due to the particular apparatus and configuration used and not due to the samples.

The average E for the half cylinder experiments (13.41 ± 2.26 GPa) was found to be between the value of c_{44} for a flat plate (2.60 ± 0.31 GPa from Kaforey et al.[8]) and $E_{//a}$ measured in compression (19.6 GPa from Archer[12]). This was expected since a half cylinder is in a mixed mode intermediate to these two cases. The edges of the samples were experiencing the situation measured by $E_{//a}$ while the center of the sample was experiencing the situation measured by three-point bending of a flat plate.

The individual PBN leaves were also mixed mode cases with the situation becoming closer to the case for a flat plate as the angular leaf span decreases and closer to the case of a half

9

cylinder as the angular leaf span increases. Generally, the effective moduli found for the individual leaves fall between the flat plate c_{33} and the effective modulus for a half cylinder.

The effective modulus for the individual leaves was hypothesized to be some functional form of the modulus for the two limiting cases (flat plate and half cylinder). It was reasonable to assume that the functional form depended on the angular leaf span, θ, so the following equation was developed and tested:

$$E_P = E_{FP}\left[1 - \sin\left(\frac{\theta}{2}\right)\right] + E_{HC}\sin\left(\frac{\theta}{2}\right) \tag{14}$$

where E_P was the predicted effective modulus, E_{FP} was the elastic modulus for the flat plate and E_{HC} was the effective modulus for a half cylinder. Figure 4 shows a plot of E_{eff} versus $\sin\left(\frac{\theta}{2}\right)$ for all of the experiments and includes the line predicted by equation (14). The angular leaf span, θ, is zero for a flat plate and pi radians (180 degrees) for a half cylinder. A paired-t test shows that there is no statistically significant difference between the predictions and the experimental results. Thus, in the future, equation (14) can be used to predict the effective modulus for a leaf of a given angular leaf span. Equation (12) can then be used to predict the spring constant for a PBN leaf of any given geometry. The spring constant was predicted to within 100 % and in the majority of the cases to within 30%.

6. Conclusions

A theoretical equation, which has a closed form solution, was derived for a cylindrical section with a line force applied at the center and simply supported at both edges. This equation is applicable to any cylindrical section under the same geometrical constraints.

10

The effective modulus was measured for half cylinders of PBN and found to be 13.41 ± 2.26 GPa. This is a mixed mode situation between the situation of three-point bending of a flat plate with the pyrolytic layers perpendicular to bending (c_{44}) and compression parallel to the pyrolytic layers ($E_{//a}$). As expected, the effective modulus found for half cylinders of PBN was between these values.

The effective moduli for individual leaves of PBN were calculated from the measured steady state force and maximum deflection values. The effective moduli for individual leaves were found to be between that of a flat plate and that of the half cylinders. The effective modulus was able to be predicted using a sine function of one half the angular leaf span, θ, to weight the modulus for a flat plate ($\theta = 0°$) and the effective modulus for a half cylinder ($\theta = 180°$).

A similar dependence on the angular leaf span would be expected for other layer structure materials. Thus, predictions of spring constants for leaves made from other pyrolytic materials could be made if the modulus for three-point bending of a flat plate with the pyrolytic layers perpendicular to bending (c_{44}) and the effective modulus for a half cylinder were known.

7. References

1. M. L. Kaforey, J. M. Bly and D. H. Matthiesen, "Void Formation in Gallium Arsenide Crystals Grown in Microgravity." J. Cryst. Growth **174**, 112-119 (1997).

2. D.H. Matthiesen and J.A. Majewski, "The Study of Dopant Segregation Behavior During the Growth of GaAs In Microgravity"; pp. 232-262 in NASA Joint Launch 1 Year Science Review, Vol. 1. NASA Conference Publication 3272, May 1994.

3. D.H. Matthiesen, M.L. Kaforey, and J.M. Bly, "Experiment XIII. The Study of Dopant

Segregation Behavior During the Growth of GaAs in Microgravity on USML-2"; pp. 293-335 in Second United States Microgravity Laboratory: One Year Report, Vol. 1. NASA TM-1998-208697, August 1998.

4. J.M. Bly, M.L. Kaforey, D.H. Matthiesen, and A. Chait, "Interface Shape and Growth Rate Analysis of Se/GaAs Bulk Crystals Grown in the NASA Crystal Growth Furnace (CGF)," J. Cryst. Growth **174**, 220-225 (1997).

5. R.S. Pease, "An X-ray Study of Boron Nitride," Acta Cryst. **5**, 356-361 (1952).

6. L. Duclaux, B. Nysten, J-P. Issi, and A.W. Moore, "Structure and Low-temperature Thermal Conductivity of Pyrolytic Boron Nitride," Phys. Rev. B **46** [6] 3362-3367 (August 1992).

7. C. W. Deeb, "Mechanical Characterization of Pyrolytic Boron Nitride (PBN) Leaf Springs," M.S. Thesis, Materials Science & Engineering (Case Western Reserve University, Cleveland, OH, 1999).

8. M. L. Kaforey, C. W. Deeb, D. H. Matthiesen, and D. J. Roth, "Elastic Moduli of Pyrolytic Boron Nitride Measured Using 3-Point Bending and Ultrasonic Testing," submitted to J. Am. Ceram. Soc. (1999).

9. B. Jager, Ph.D. Thesis, Universit□ de Grenoble (1977) as cited in L. Duclaux, B. Nysten, J-P. Issi, and A.W. Moore, "Structure and Low-temperature Thermal Conductivity of Pyrolytic Boron Nitride," Phys. Rev. B **46** [6] 3362-3367 (August 1992).

10. B.T. Kelly, "The Anisotropic thermal expansion of boron nitride II. Interpretation by the semi-continuum model," Phil. Mag. **32**, 859-867 (1975).

11. Union Carbide Corporation (Advanced Ceramics Corporation), "Boralloy: Pyrolytic Boron Nitride." Corporate literature (1987).

12. N.J. Archer, "The Preparation and Properties of Pyrolytic Boron Nitride" pp. 167-180 in

"High Temperature Chemistry of Inorganic Ceramic Materials: Proceedings of a

Conference," Chemical Society Special Publication Number 30 (1977).

13. W.C. Young, *Roark's formulas for stress and strain*, 6th ed. (McGraw-Hill, New York,

1989).

14. S. Timoshenko and S. Woinowsky-Krieger, *Theory of Plates and Shells*, 2nd ed. (McGraw-

Hill, New York, 1959).

15. C. A. P. Castigliano, *Théorème de l'équilibre des systèmes élastiques et ses applications*,

Paris, 1879. English translation in E. S. Andrews, *The Theory of Equilibrium of Elastic*

Systems and Its Applications, Dover Publications, Inc., New York, 1966.

16. F. P. Beer and E. R. Johnston, Jr., *Vector Mechanics for Engineers*, 4th ed., McGraw-Hill,

New York, 1984.

17. N. Naito and C. H. Hsueh, "Residual stress and strain in pyrolytic boron nitride resulting

from thermal anisotropy," J. Mat. Sci. **23**, 1901-1905 (1988).

8. Figure Captions

Figure 1. Schematic showing (a) end view of pyrolytic boron
nitride (PBN) cylinder of radius, r, and cylindrical section
of width, w, and (b) individual leaf of thickness, h, and
depth, b, with force applied at centerline.

Figure 2. Typical force versus deflection chart recording for a half
cylinder experiment. For this case, maximum deflection, d
= 0.2 mm and steady state load, P = 2.38 lbf = 10.6 N
(0.500 lbf = 2.224 N).

Figure 3. Typical force versus deflection chart recording for an
individual leaf experiment. For this case, maximum
deflection, d = 0.28 mm and steady state load, P = 0.314 lbf
= 1.40 N (0.500 lbf = 2.224 N).

Figure 4. Plot of E_{eff} versus $\sin\left(\dfrac{\theta}{2}\right)$ for all individual leaf

experiments. Also included is a line showing the predictions for E_P calculated from equation (14).

Table 1. Load versus deflection results for PBN half cylinders.

Test #	Radius, r	Width, w	Thickness, h	Depth, b	Angular leaf span, θ	Spring constant, $k = P/d$	Effective modulus, E_{eff}
	Mm	mm	mm	mm	radians	N/mm	GPa
1	10.80	21.59	0.76	12.95	3.08	22.99	10.89
2	9.84	19.69	0.71	16.31	3.14	34.04	11.82
3	15.65	31.29	1.02	33.83	3.09	60.76	14.02
4	15.60	31.19	0.91	33.02	3.09	52.22	16.77
5	15.65	31.29	1.02	15.62	3.09	27.98	13.57
							Average: 13.41 ±2.26

Table 2. Load versus deflection results for individual PBN leaves.

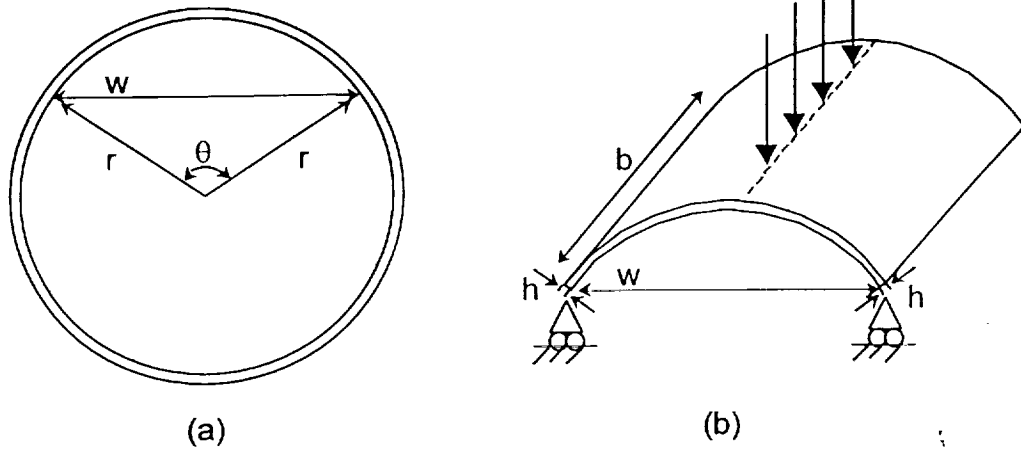| Test #	Radius, r	Width, w	Thickness, h	Depth, b	Angular leaf span, θ	Spring constant, $k = P/d$	Effective modulus, E_{eff}
	mm	mm	mm	mm	radians	N/mm	GPa
1	29	15	0.394	15	0.52	8.43	8.15
2	28.6	15.2	0.851	15.2	0.52	46.96	4.49
3	64.8	15.2	0.635	15.2	0.23	31.32	7.09
4	39.4	15.2	0.508	15.2	0.39	14.47	6.45
5	64.8	15.2	0.356	15.2	0.23	4.31	5.56
6	64.8	15.2	0.870	15.2	0.23	50.53	4.46
7	64.8	15.2	0.864	15.2	0.23	70.44	6.34
8	39.4	15.2	0.508	15.2	0.39	20.42	9.10
9	64.8	15.2	0.546	15.2	0.23	29.69	10.57
10	28.6	15.2	0.229	15.2	0.52	1.98	9.76
11	28.6	15.2	0.838	15.2	0.52	84.74	8.48
12	64.8	15.2	0.254	15.2	0.23	1.01	3.56
13	10.8	10.0	0.762	12.9	0.96	53.54	2.35
14	15.7	8.3	1.016	15.6	0.54	142.53	1.25
15	15.7	23.2	1.016	15.6	1.67	60.69	11.87
16	10.8	6.6	0.762	12.9	0.62	52.48	0.67
17	10.8	15.9	0.762	12.9	1.66	43.46	7.90
18	15.7	17.2	1.016	15.6	1.17	94.19	7.46

Figure 1. Schematic showing (a) end view of pyrolytic boron
nitride (PBN) cylinder of radius, r, and cylindrical section
of width, w, and (b) individual leaf of thickness, h, and
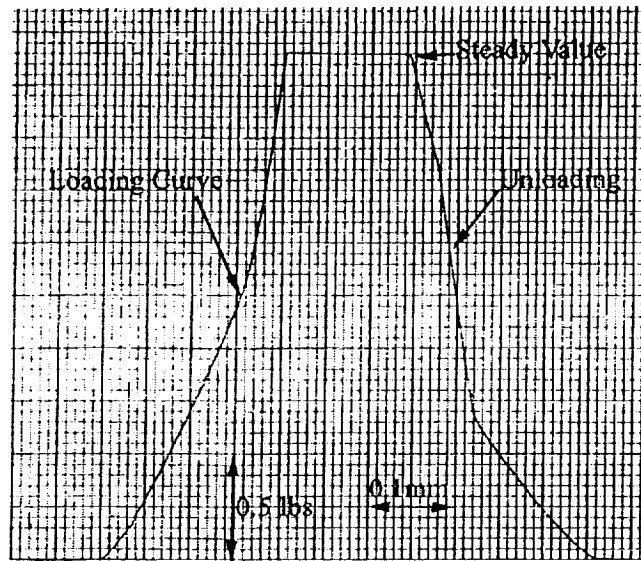depth, b, with force applied at centerline.

Figure 2. Typical force versus deflection chart recording for a half
cylinder experiment. For this case, maximum deflection, d
= 0.2 mm and steady state load, P = 2.38 lbf = 10.6 N
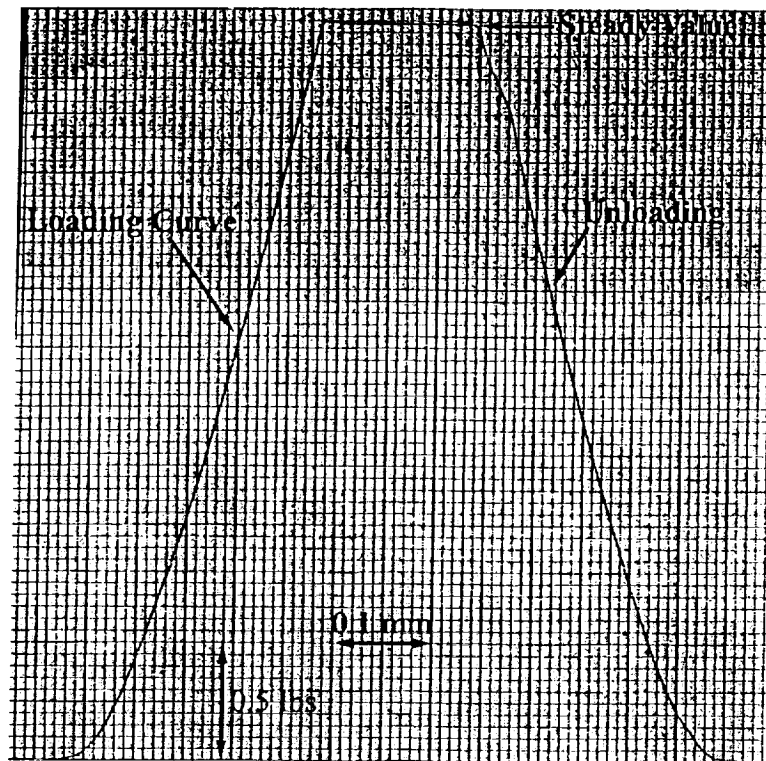(0.500 lbf = 2.224 N).

Figure 3. Typical force versus deflection chart recording for an
individual leaf experiment. For this case, maximum
deflection, $d = 0.28$ mm and steady state load, $P = 0.314$ lbf
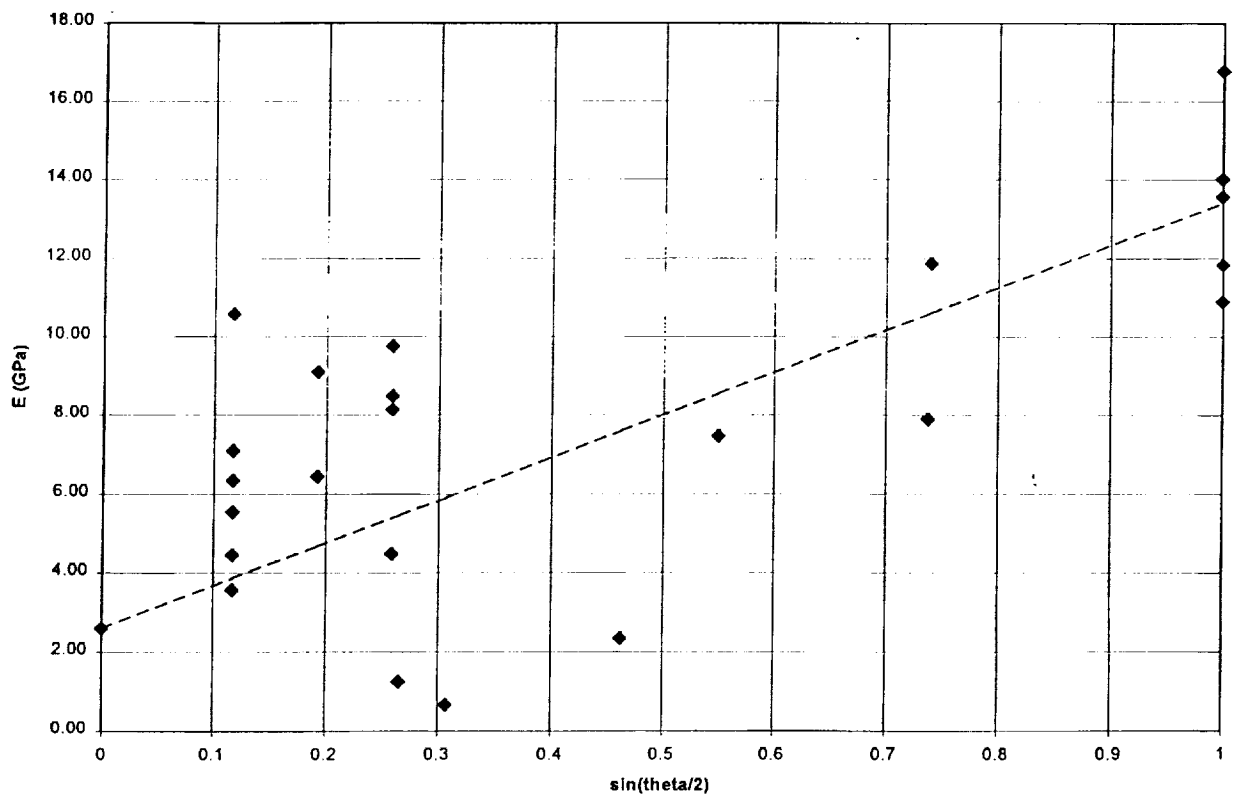$= 1.40$ N (0.500 lbf $= 2.224$ N).

Figure 4. Plot of E_{eff} versus $\sin\left(\dfrac{\theta}{2}\right)$ for all individual leaf experiments. Also included is a line showing the predictions for E_P calculated from equation (14).